

Supplementary Information

Crystallographic Analyses of Isoquinoline Complexes Reveal a New Mode of Metallo- β -Lactamase Inhibition

Guo-Bo Li,^{ab} Jürgen Brem,^{a*} Robert Lesniak,^a Martine I. Abboud,^a Christopher T. Lohans,^a Ian J. Clifton,^a Sheng-Yong Yang,^b Juan-Carlos Jiménez-Castellanos,^c Matthew B. Avison,^c James Spencer,^c Michael A. McDonough,^a and Christopher J. Schofield,^{a*}

^a *Department of Chemistry, University of Oxford, 12 Mansfield Road, Oxford, OX1 3TA, United Kingdom.*

^b *Key Laboratory of Drug Targeting and Drug Delivery System of Ministry of Education, West China School of Pharmacy and State Key Laboratory of Biotherapy, Sichuan University, Chengdu, 610041, China.*

^c *School of Cellular and Molecular Medicine, Biomedical Sciences Building, University of Bristol, Bristol BS8 1TD, United Kingdom.*

*Correspondence: christopher.schofield@chem.ox.ac.uk (C.J. Schofield) or jurgen.brem@chem.ox.ac.uk (J. Brem).

Contents

Supplementary Experimental Section	2
SE. 1. NMR Experiments	2
SE. 2. Chemical Synthesis	2
SE. 3. Inhibition Assays	6
SE. 4. Crystallographic Analyses	6
SE. 5. Microbiological Testing	7
Supplementary Figures	8
Supplementary Tables	25
Reference	28

Supplementary Experimental Section

SE. 1. NMR Experiments.

General. Nuclear Magnetic Resonance (NMR) spectra were recorded with a Bruker AVIII 600 MHz NMR spectrometer equipped with a BB-¹⁹F/¹H Prodigy N₂ cryoprobe using 5 mm diameter NMR tubes (Norell). Data were processed with Bruker 3.1 software.

¹H Excitation Sculpting Suppression NMR Experiments. For ¹H excitation sculpting suppression NMR experiments, spectra were typically obtained using 16 scans and a relaxation delay of 1 s. A 2 ms Sinc pulse was used for water suppression. The assay mixture contained 20 μM di-Zn(II)-VIM-5 or *apo*-VIM-5 supplemented with 400 μM of the compound to be studied buffered with 50 mM Tris-D₁₁ (pH 7.5) and 0.02 % NaN₃ in 90 % H₂O and 10 % D₂O.

wLOGSY NMR experiments. water-Ligand Observed Gradient Spectroscopy (wLOGSY) experiments were conducted using the pulse sequence described by Dalvit *et al.*¹ Typical experimental parameters were as follows: mixing time, 1 s; relaxation delay, 2 s; number of transients, 400. Solvent excitation was achieved using a 16 ms 180 degree selective rectangular shape pulse with 1000 points (Squa100.1000) set at the H₂O frequency. Water suppression was achieved by a 2 ms Sinc pulse (Sinc1.1000) pulse at the H₂O frequency. The assay mixture contained 20 μM di-Zn(II)-VIM-5 or *apo*-VIM-5 supplemented with 400 μM of the compound to be studied buffered with 50 mM Tris-D₁₁ (pH 7.5) and 0.02 % NaN₃ in 90 % H₂O and 10 % D₂O.

¹H CPMG NMR experiments. Typical experimental parameters for Carr-Purcell-Meiboom-Gill (CPMG) NMR spectroscopy were as follows: total echo time, 40 ms; relaxation delay, 2 s; number of transients, 128. The PROJECT-CPMG sequence (90°x-[τ-180°y-τ-90°y-τ-180°y-τ] *n*-acq) as described by Aguilar *et al.*² was applied. Water suppression was achieved by pre-saturation. Data were processed with Bruker 3.1 software. Prior to Fourier transformation, data were multiplied with an exponential function with a 0.3-Hz line broadening. Titrations were carried out and dissociation constant (*K_D*) values fitted as reported³.

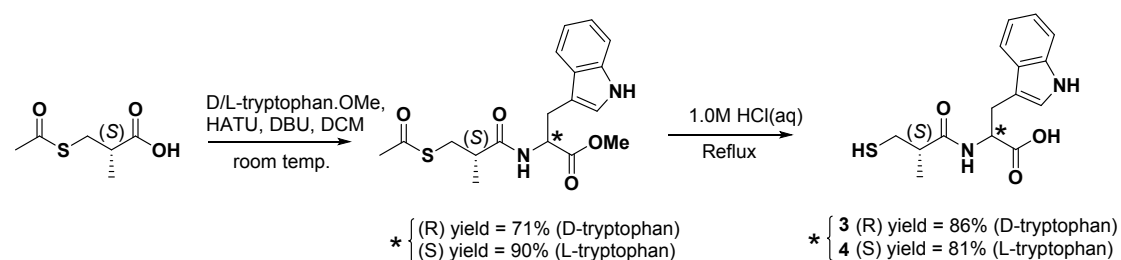
SE. 2. Chemical Synthesis.

All chemicals including reagents and solvents were from Sigma-Aldrich (Dorset, U.K.) and used without further purification. Solvents used were of HPLC purity and used for reactions chromatography and work-ups. Aqueous solutions were made using de-ionized water. Thin layer chromatography (TLC) was carried out using Merck (Darmstadt, Germany) silica gel 60 F254 TLC plates. TLC visualization was carried

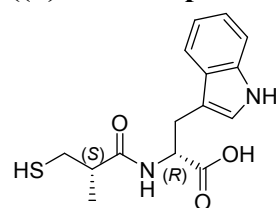
out under UV light, and stained with one of three stains; ninhydrin, potassium permanganate or anisaldehyde. Chromatographic purifications were carried out using a Biotage (Uppsala, Sweden) Isolera One or Biotage SP4 flash purification system using Biotage pre-packed SNAP columns (FCC). Reactions were monitored using an Agilent (Cheshire, U.K.) 1200 series, 6120 quadrupole LC/MS machine and a Merck Chromolith Performance RP-18 HPLC column. Deuterated solvents were from Sigma-Aldrich. ^1H NMR spectra were obtained using a Bruker AVANCE AV400 (400MHz) NMR spectrometer. All signals are described in δ ppm with multiplets being denoted as singlet, doublet, triplet, quartet and multiplet using the abbreviations s, d, t, q, and m respectively. Chemical shifts were referenced using residual solvent peaks with coupling constants, J , reported in hertz (Hz) to an accuracy of 0.5 Hz. To obtain high-resolution mass spectrometry data (HR-MS) a Bruker MicroTOF instrument using an ESI source and Time of Flight (TOF) analyser was used. Mass spectrometry data (m/z) are represented as a ratio of mass to charge in Daltons. A Bruker Tensor 27 instrument was used to obtain Fourier transform infrared spectra (FT-IR). Spectroscopic grade solvents and a Perkin Elmer 241 Polarimeter were used to obtain optical rotations.

Scheme S1.

Compounds **3** and **4** were synthesized via the route shown in Scheme S1.



((S)-3-Mercapto-2-methylpropanoyl)-D-tryptophan (**3**)

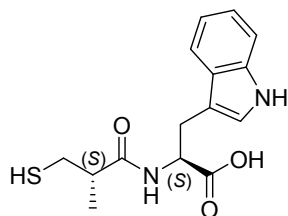


Methyl ((S)-3-(acetylthio)-2-methylpropanoyl)-D-tryptophan (250mg, 0.69 mmol) was dissolved in 1.0M $\text{HCl}_{(\text{aq})}$ (2.7ml). The mixture was heated until reflux and stirred overnight. The reaction mixture was allowed to cool to room temperature before being diluted with 10ml H_2O . The reaction mixture was then extracted with EtOAc (3 x 15ml), after which all organic fractions were collected and dried over MgSO_4 , filtered and concentrated before being purified by FCC eluting with DCM (CH_2Cl_2)/(MeOH + 0.1% AcOH), 95:5. The appropriate fractions were collected and concentrated to

dryness to give **3** as a slightly yellow oil, several triturations using Et₂O, produced a white, waxy, amorphous solid (181mg, 0.59mmol, 86%).

¹H NMR (CD₃OD, 400 MHz) δ = 7.57 (1H, dt, *J*=7.9, 1.1 Hz, *Ar*), 7.32 (1H, dt, *J*=8.1, 1.0 Hz, *Ar*), 7.11 – 7.05 (2H, m, 14, *Ar*), 7.03 – 6.98 (1H, m, *Ar*), 4.75 (1H, dd, *J*=8.6, 5.1 Hz, -NHCHCH₂-), 3.37 (1H, ddd, *J*=14.5, 4.8, 0.8 Hz, -NHCHC(H_AH_B)-), 3.17 (1H, dd, *J*=14.8, 8.6 Hz, -NHCHC(H_AH_B)-), 2.68 (1H, dd, *J*=13.2, 7.9 Hz, HSC(H_AH_B)CH-), 2.52 – 2.43 (1H, m, HSCH₂CH-), 2.38 (1H, ddt, *J*=13.2, 5.9, 1.3 Hz, HSC(H_AH_B)CH-), 1.00 (3H, d, *J*=6.9 Hz, HSCH₂CHCH₃) ppm. ¹³C NMR (CD₃OD, 101 MHz) δ = 177.41, 175.23, 138.02, 128.84, 124.34, 122.38, 119.75, 119.27, 112.23, 111.13, 54.52, 45.73, 28.52, 28.45, 17.34 ppm. FT-IR ν_{max} (film) 1680, 1578, 1518, 1454, 1348, 1288, 1202, 739 cm⁻¹. [α]_D²⁵ = -30.0° (c = 0.13 in MeOH). HRMS (ESI-TOF) calcd for C₁₅H₁₈N₂O₃NaS [M+Na]⁺: 329.0930, found: 329.0925.

((S)-3-Mercapto-2-methylpropanoyl)-L-tryptophan (**4**)



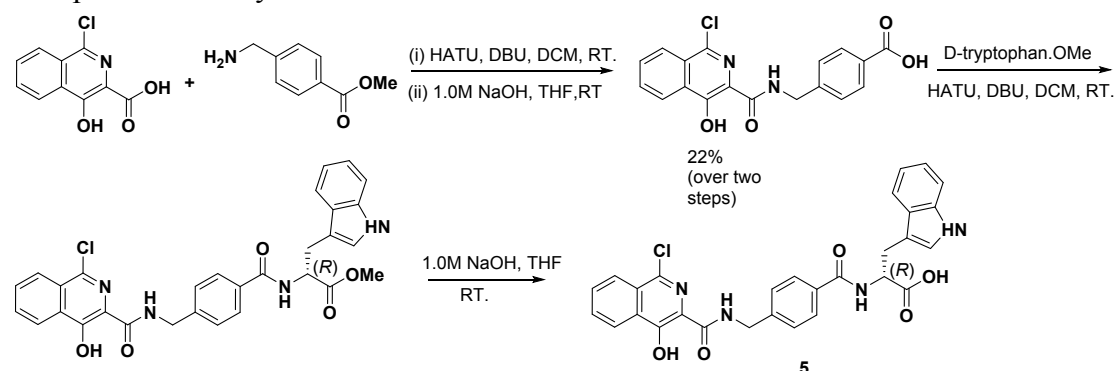
To round bottom flask containing Methyl ((S)-3-(acetylthio)-2-methylpropanoyl) -L-tryptophanate (250mg, 0.82mmol) was added 1.0M HCl_(aq) (2.7ml). The mixture was allowed to stir under reflux overnight after which the reaction mixture was diluted with H₂O (10ml). The resulting solution was extracted with EtOAc (3 x 15ml). The organic layers were combined, dried over MgSO₄, filtered and concentrated to dryness before being purified by FCC using an isocratic gradient of DCM/(MeOH + 0.1% AcOH), 95:5. The appropriate fractions were collected and evaporated *in vacuo* to yield **4** as a clear, slightly yellow oil. Several triturations with Et₂O, liberated a white, waxy solid (171 mg, 0.56 mmol, 81%).

¹H NMR (CD₃OD, 400 MHz) δ = 7.60 (1H, dt, *J*=7.8, 1.1 Hz, *Ar*), 7.31 (1H, dt, *J*=8.1, 1.0 Hz, *Ar*), 7.14 (1H, s, *Ar*), 7.11 – 7.05 (1H, m, *Ar*), 7.03 – 6.98 (1H, m, *Ar*), 4.79 (1H, dd, *J*=8.8, 5.0 Hz, -NHCHCH₂-), 3.37 (1H, ddd, *J*=14.7, 4.9, 0.9 Hz, -NHCHC(H_AH_B)-), 3.17 (1H, ddd, *J*=14.7, 8.8, 0.7 Hz, -NHCHC(H_AH_B)-), 2.33 (1H, ddt, *J*=12.6, 4.9, 1.2 Hz, HSC(H_AH_B)CH-), 2.58 – 2.43 (2H, m, HSC(H_AH_B)CH-, HSCH₂CH-), 1.11 (3H, d, *J*=6.7 Hz, HSCH₂CHCH₃) ppm. ¹³C NMR (CD₃OD, 101 MHz) δ = 177.34, 175.26, 138.04, 128.79, 124.53, 122.37, 119.76, 119.33, 112.23, 111.09, 54.35, 45.80, 28.58, 28.37, 17.48 ppm. FT-IR ν_{max} (film) 1694, 1587, 1520, 1487, 1385, 1346, 1165, 964, 943, 785, 741 cm⁻¹. [α]_D²⁵ = -18.5° (c = 0.18 in MeOH).

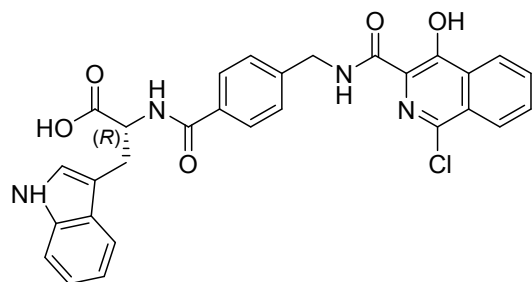
HRMS (ESI-TOF) calcd for C₁₅H₁₈N₂O₃NaS [M+Na]⁺: 329.0930, found: 329.0930.

Scheme S2.

Compound **5** was synthesized via the route in Scheme S2.



(4-((1-Chloro-4-hydroxyisoquinoline-3-carboxamido)methyl)benzoyl)-D-tryptophan (**5**)



Methyl (4-((1-chloro-4-hydroxyisoquinoline-3-carboxamido)methyl)benzoyl)-D-tryptophanate (86.9 mg, 0.16 mmol) was dissolved in THF (2 ml) before 1.0M aqueous NaOH (0.47 ml) was added. The mixture was then stirred overnight at room temperature before being neutralized with 1.0M aqueous HCl. The resulting solution was extracted with EtOAc (3 x 5 ml) and the organic layers combined, dried over MgSO₄, filtered and concentrated before being purified by flash column chromatography (95:5, CH₂Cl₂/(MeOH + 0.1% AcOH)) to give the desired compound **5** (79.5 mg, 0.15 mmol, 92%). ¹H NMR(CD₃OD, 400 MHz) δ = 9.01 (1H, s, -CONHCH₂-), 8.18 – 8.12 (1H, m, Ar), 8.09 – 8.04 (1H, m, Ar), 7.70 (2H, p, *J* = 3.5 Hz, Ar), 7.64 – 7.60 (2H, m, Ar), 7.57 (1H, dt, *J* = 8.0, 0.9 Hz, Ar), 7.32 (2H, dt, *J* = 8.0, 2.0 Hz, Ar), 7.30 – 7.26 (1H, m, Ar), 7.10 (1H, s, -C=CHNH), 7.03 (1H, ddd, *J* = 8.0, 7.0, 1.0 Hz, Ar), 6.95 (1H, ddd, *J* = 8.0, 7.0, 1.0 Hz, Ar), 4.95 – 4.91 (10H, m, -CONHCH-), 4.54 (2H, s, -NHCH₂-), 3.47 (1H, dd, *J* = 14.7, 5.0 Hz, -CHC(H_A,H_B)-), 3.36 – 3.26 (1H, m, -CHC(H_A,H_B)-) ppm. ¹³C NMR (CD₃OD, 101 MHz) δ = 175.3, 175.2, 170.3, 169.7, 155.5, 143.7, 140.3, 138.0, 134.1, 132.0, 131.0, 130.2, 128.8, 128.6, 128.5, 127.1, 124.4, 124.0, 122.4, 119.9, 119.2, 112.3, 111.1, 43.3, 28.3, 20.7 ppm. FT-IR *v*_{max} (film) 1719, 1620, 1483, 1437, 1319, 969, 744 cm⁻¹. [α]_D²⁵ = +25.7° (c = 0.98 in MeOH). HRMS (ESI-TOF) calcd for C₂₉H₂₄ClN₄O₅[M+H]⁺: 543.1430, found: 543.1428.

SE. 3. Inhibition Assays.

Except where noted, recombinant forms of VIM-2, VIM-5, VIM-1, NDM-1, SPM-1, and BcII, and IMP-1 MBLs were produced in *Escherichia coli*; assays were carried out as described.⁴ The IC₅₀ values of all the compounds against B1 MBLs including VIM-2, VIM-5³, VIM-1, NDM-1, SPM-1, and BcII, and IMP-1 were determined using the same method as described previously.⁴ The inhibitory activities of these compounds against CphA (B2 MBL)⁵ and L1 (B3 MBL)⁶ were determined using meropenem and nitrocefin, respectively. The IC₅₀ values were determined for compounds showing inhibition >30% at 100 μM. The details regarding enzyme concentrations please see our previous works.

SE. 4. Crystallographic Analyses.

Structures of VIM-5 in complex with inhibitors **1** and **2** were obtained by co-crystallization; Structures of VIM-2:**3** and VIM-2:**4** were obtained by soaking. Purified VIM-5 proteins were freshly prepared to a concentration of 20.89 mg/mL in crystallization buffer (50 mM HEPES-NaOH, pH 7.5, 100 mM NaCl), followed by adding 1 mM tris(2-carboxyethyl)phosphine (TCEP) and 5 mM inhibitor. The protein-inhibitor mixtures were co-crystallized using the sitting drop vapour diffusion method in 96 well 3-subwell Intelliplates® (Art Robbins). The reservoir buffer for growing crystals were from commercially available crystallization conditions (PACT and INDEX). The crystals were cryoprotected by diluting the crystal growth well solution to 25% (v/v) glycerol to make a cryo-solution which was then added to the crystallisation drop 10:1, crystals were harvested in nylon loops and flash-cooled in liquid nitrogen. Data were collected on single crystals in-house or at the Diamond Light Source synchrotron beamlines. Initial phases were obtained by molecular replacement (MR) using PHASER⁷ within PHENIX⁸ and the structure of VIM-5 (PDB code: 5A87)³ as a search model. Crystallization of VIM-2 and soaking with **3** or **4** were carried out as previously described.^{9, 10} Crystallographic structure refinement was carried out by iterative rounds of model building using Coot¹¹ and maximum likelihood restrained refinement using PHENIX. Crystallization conditions are in Table S2, and data collection and refinement statistics are in Table S3.

Protein Structure Accession Number. Coordinates and structure factors for structures of VIM-5:**1**, VIM-5(Oxidized):**1**, VIM-5(Oxidized):**2**, VIM-2:**3**, and VIM-2:**4** have been deposited in the Protein Data Bank with the accession codes of 5N58, 5NAI, 5N55, 5N4S and 5N4T, respectively (Table S3).

SE. 5. Microbiological Testing

Test bacteria were clinical isolates of *Escherichia coli* (a urinary tract isolate kindly provided by Dr Mandy Wootton, Public Health Wales, Cardiff), *Enterobacter aerogenes* (a paediatric bloodstream isolate)¹² and *Klebsiella pneumoniae* Ecl8.¹³ Subclass B1 β -lactamase genes were cloned alongside their native hybrid integron promoter: *bla*_{IMP-1} (sequence as in Genbank accession number AP012280.1) was PCR amplified from a *Pseudomonas aeruginosa* clinical isolate (from Dr Mark Toleman, Cardiff University) using primers IntpCH1 F- 5'-ACCCAGTGGACATAAGCCTG-3' and impR 5'-AGCGAAGTTGATATGTATTGTG-3'. *bla*_{VIM-1} (sequence as in accession number GQ422829.1) was amplified from a *K. pneumoniae* clinical isolates (from Prof Tim Walsh, Cardiff University) using primers IntpCH1 (above) and vimR 5'- TCTGCTACTCGGCGACTGAG-3'. Both amplicons were TA-cloned into pCR2.1-TOPO (Invitrogen) and subcloned using EcoRI into pSU18.¹⁴ Recombinant plasmids, or pSU18 as control, were used to transform the clinical isolates to chloramphenicol resistance via electroporation, as standard for laboratory *E. coli* strains. MIC analysis was performed using the standard CLSI microtitre assay protocol¹⁵ using Muller-Hinton Broth in the presence or absence of inhibitor or DMSO vehicle (1% (v/v)). Resistance/susceptibility was assigned by reference to CLSI clinical breakpoints.¹⁶

Supplementary Figures

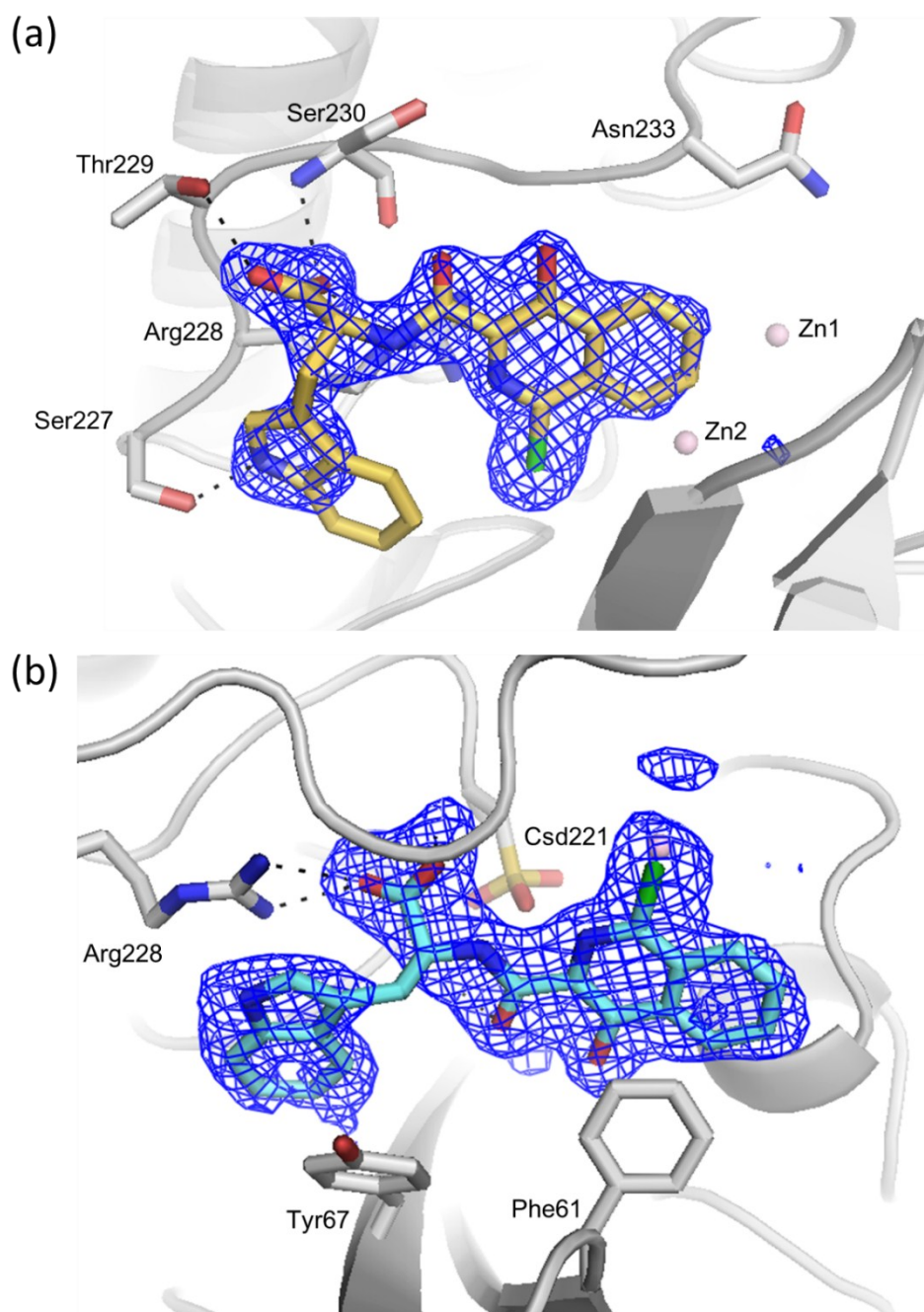


Fig. S1 Binding modes of 1 and 2 as defined by electron density maps. Structures of (a) VIM-5:1 (PDB ID: 5N58) and (b) VIM-5:2 (PDB ID: 5N55) (protein and compound colors and representations as in Fig. 2) with mF_o-DF_c electron density (OMIT maps) around 1 and 2 (blue mesh, contoured to 3σ) calculated from the final refined model without ligand present.

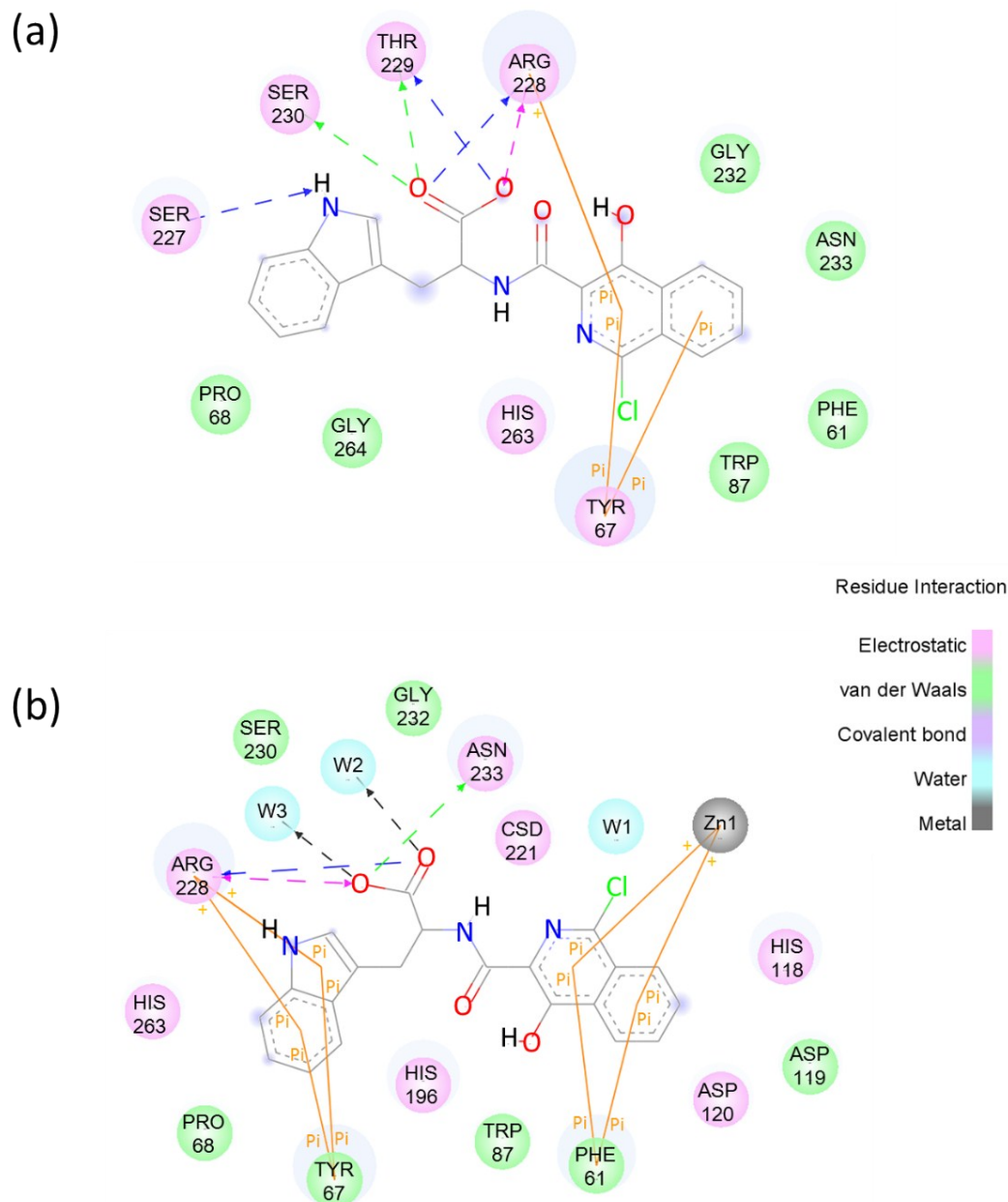


Fig. S2 Protein-ligand interactions between 1 and 2 and VIM-5 defined using the Discovery Studio Visualizer. Compounds 1 and 2 display different interactions with the VIM-5 active site residues. The carboxylate of 1 is positioned to make hydrogen-bonding and electrostatic interactions with Ser227, Arg228, Thr229, and Ser230, and its isoquinoline is positioned to form π - π stacking interactions with Tyr67 and cation- π interactions with Arg228. The carboxylate of 2 is positioned to form hydrogen bonds with Arg228 and Asn233, and its isoquinoline and indole moieties are positioned to make π - π stacking interactions with Phe61 and Try67, respectively.

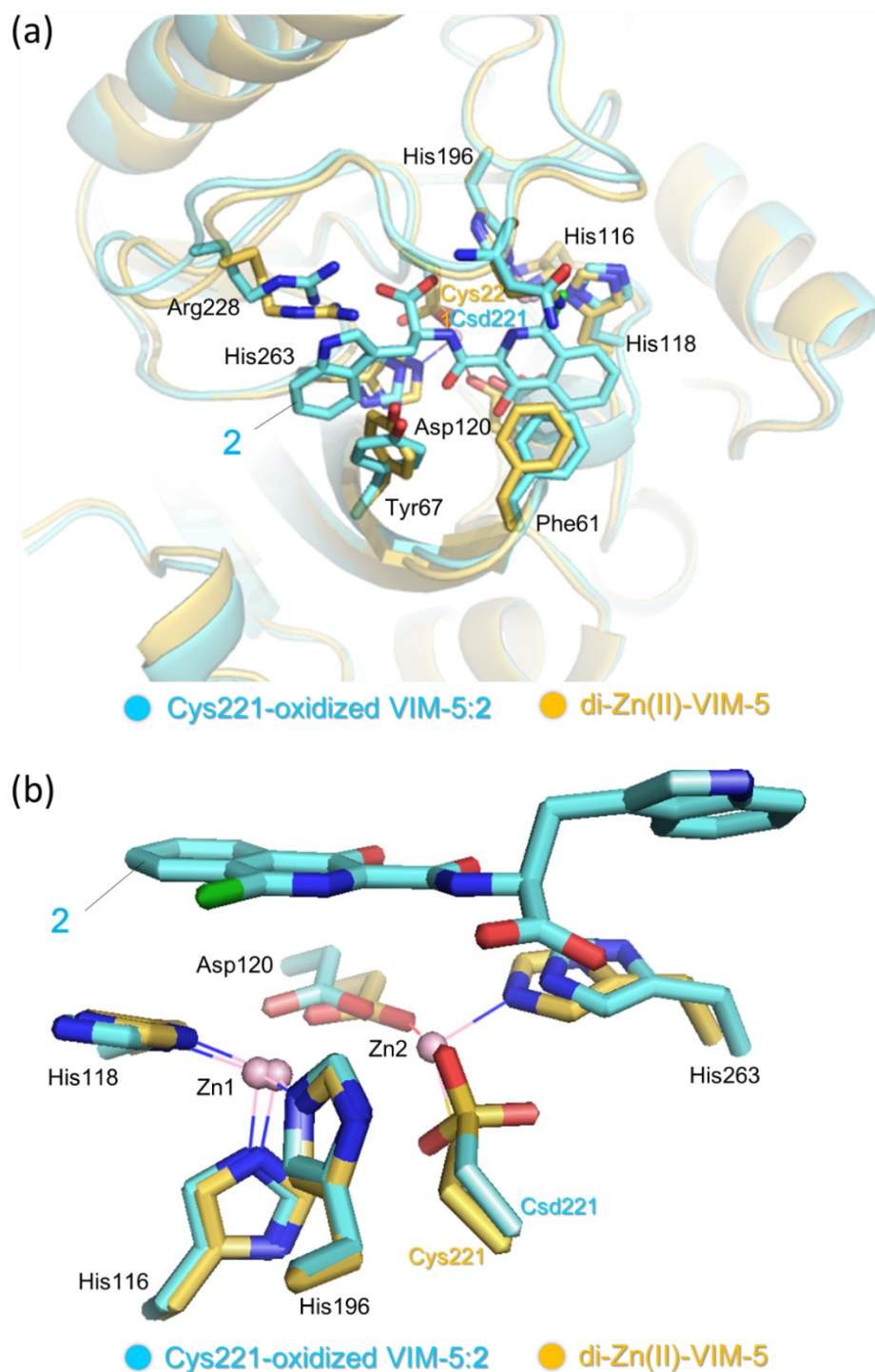


Fig. S3 Comparison of di-Zn(II) and Cys221-oxidized form of VIM-5 structures.

(a) Superimposition of the VIM-5:2 complex structure (PDB ID: 5N55) with the di-Zn(II) VIM-5 structure (PDB ID: 5A87)³ showed that both have the same protein folds and all the active site residues are in consistent position and conformation. (b) There are slight difference between the oxidized VIM-5:2 and di-Zn(II) VIM-5 structure in the active site, e.g. the residues ligated with Zn2 including Cys221 (Csd221 is the oxidized form of Cys221), Asp120 and His263.

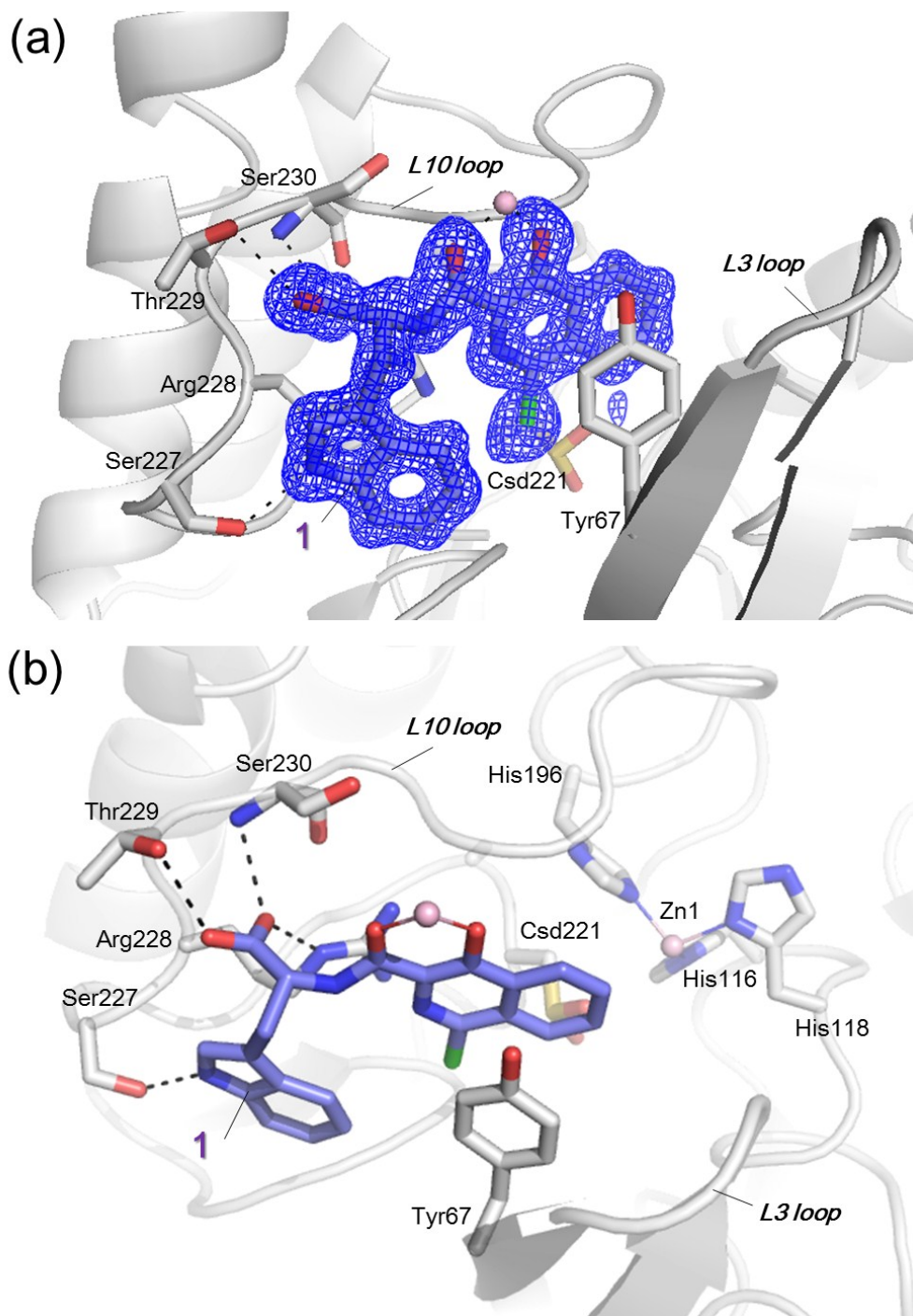


Fig. S4 Binding mode of 1 to the cysteine-24 oxidized form of VIM-5. (a) Structure of **1** in complex with the oxidized VIM-5 form (PDB ID: 5NAI) with the mF_o-DF_c electron density (OMIT maps) around **1** (blue mesh, contoured to 3σ) calculated from the final refined model without ligand present. (b) **1** binds to the L10 and L3 loop of VIM-5 via hydrogen-bonding interactions with Ser227, Arg228, Thr229, and Ser230, and π - π stacking interactions with Tyr67.

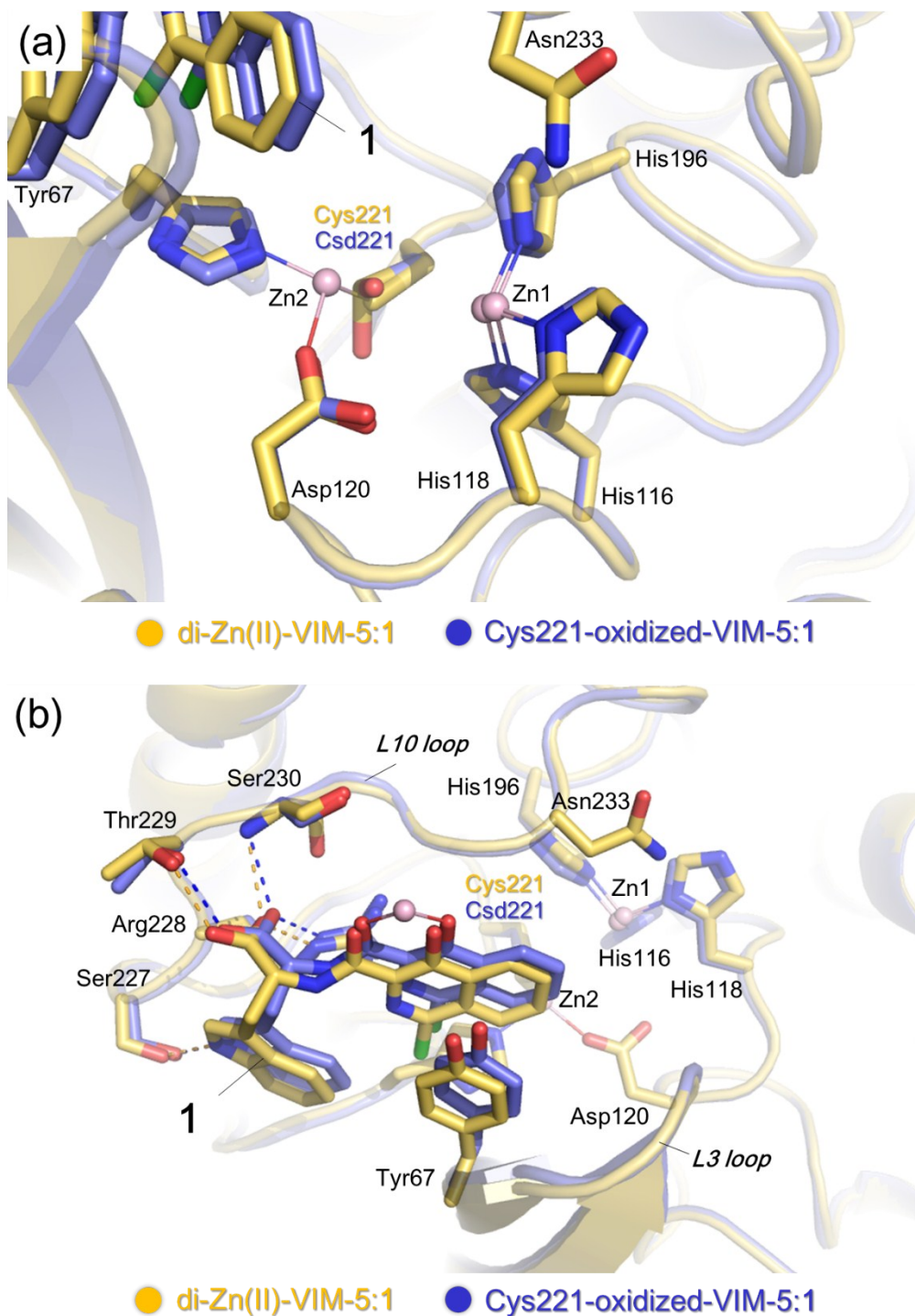


Fig. S5 Comparison of structures of **1 with di-Zn(II)-VIM-5 and Cys221-oxidized form of VIM-5.** (a) The di-Zn(II)-VIM-5 (PDB ID: 5N58) and Cys221 oxidized VIM-5 (PDB ID: 5NAI) have the same folds and all active site residues are in consistent positions and conformations. (b) **1** has the same binding mode in these two structures. These results thus indicate **1** has the same binding mode to the di-Zn(II) and oxidized structures.

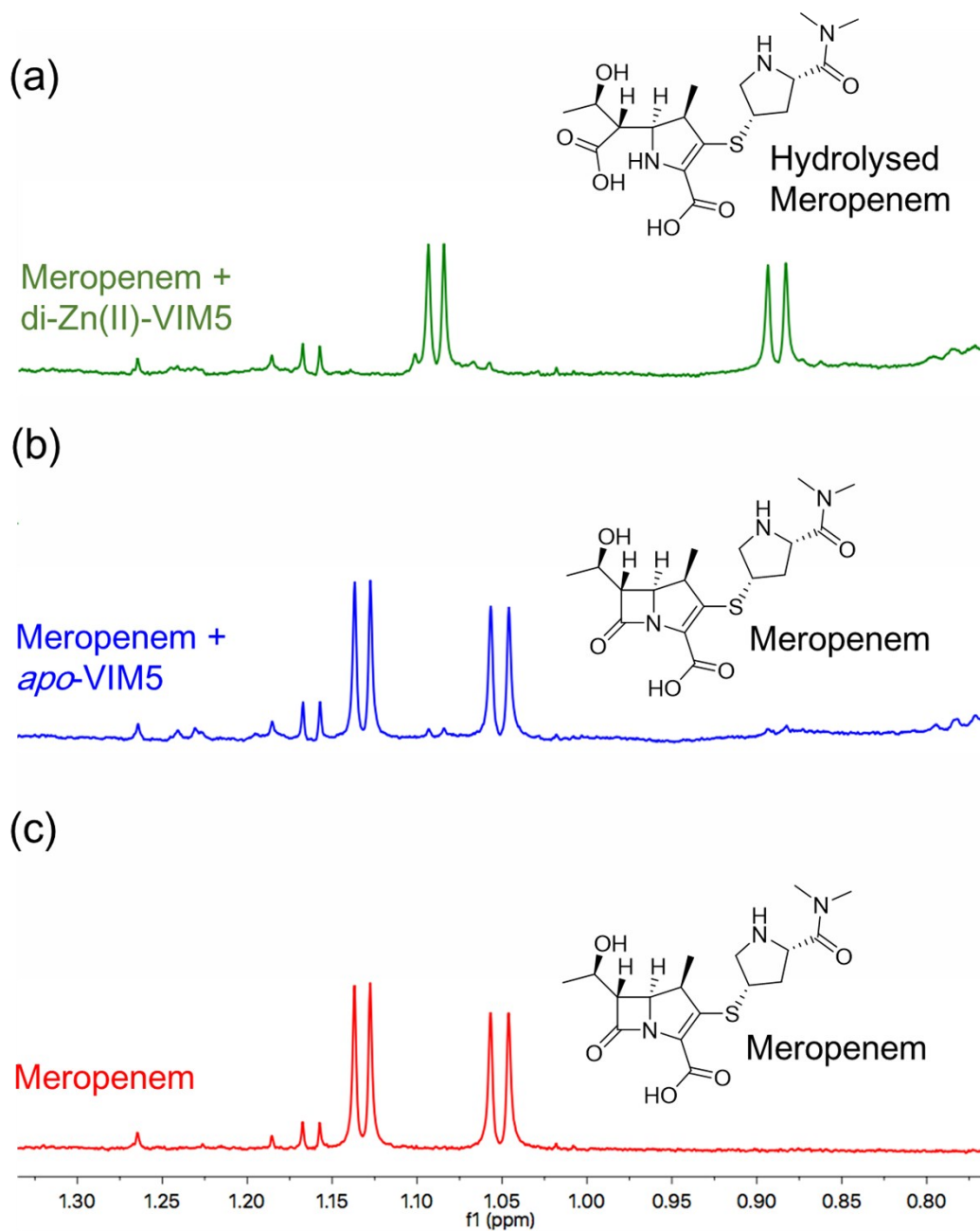


Fig. S6 ^1H NMR analyses show that *apo*-VIM-5 protein is unable to hydrolyze meropenem. (a) ^1H NMR studies of meropenem to catalytically active di-Zn(II)-VIM-5 protein. (b) ^1H NMR studies of meropenem to the *apo*-VIM-5 protein. (c) ^1H NMR of meropenem only. Assay mixtures contained 10 μM di-Zn(II)-VIM-5 or 10 μM *apo*-VIM5, and 100 μM meropenem buffered with 50 mM Tris- D_{11} pH 7.5, in 90% H_2O and 10% D_2O . Blue traces correspond to the compound only and red traces correspond to the compound in the presence of *apo*-VIM-5

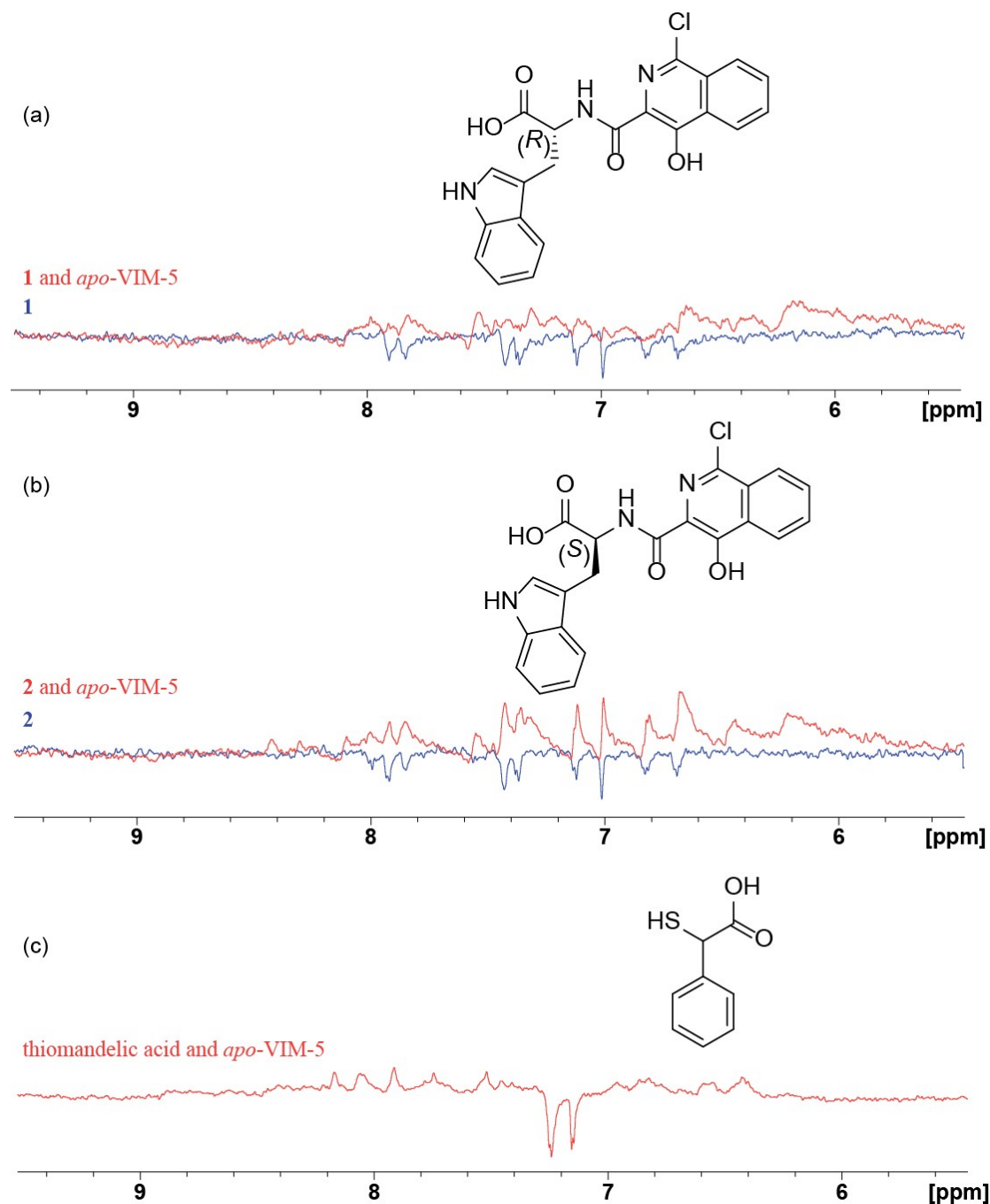


Fig. S7 Binding studies of 1 (a), 2 (b), and thiomandelic acid (c) to apo-VIM-5 analysed by wLOGSY NMR studies. The results show binding of 1 and 2 to apo-VIM-5; by contrast no binding of thiomandelic acid was observed to apo-VIM-5. Assay mixtures contained 20 μM apo-VIM-5 supplemented with 400 μM of the compound to be studied buffered with 50 mM Tris- D_{11} (pH 7.5) and 0.02 % NaN_3 in 90 % H_2O and 10 % D_2O .

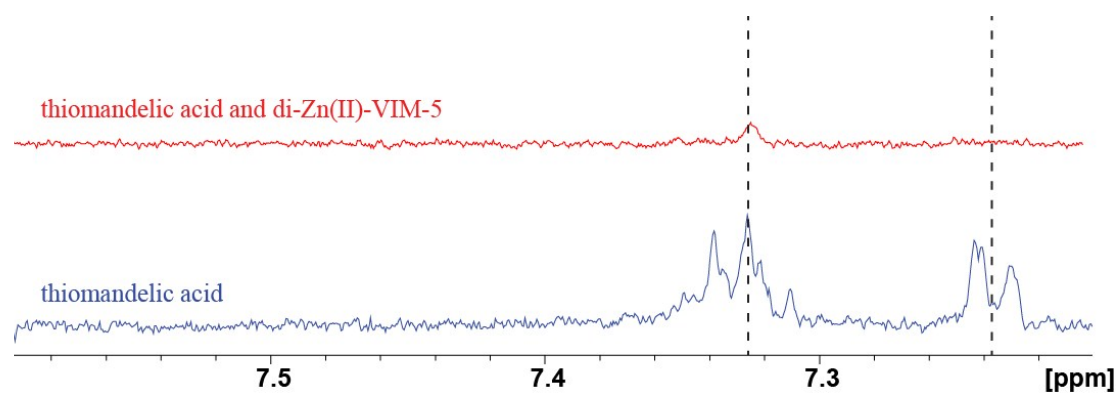


Fig. S8 Binding studies of thiomandelic acid to di-Zn(II)-VIM-5 analysed by ¹H CPMG. The assay mixture contained 50 μ M thiomandelic acid (blue trace), buffered with 50 mM Tris-D₁₁, pH 7.5, and 0.02 % NaN₃ in 90 % H₂O and 10 % D₂O, supplemented with 50 μ M di-Zn(II)-VIM-5 (red trace). The reduction in signal intensities of thiomandelic acid peaks (black dots) upon addition of di-Zn(II)-VIM-5 suggests that it is a moderate to strong binder to di-Zn(II)-VIM-5.

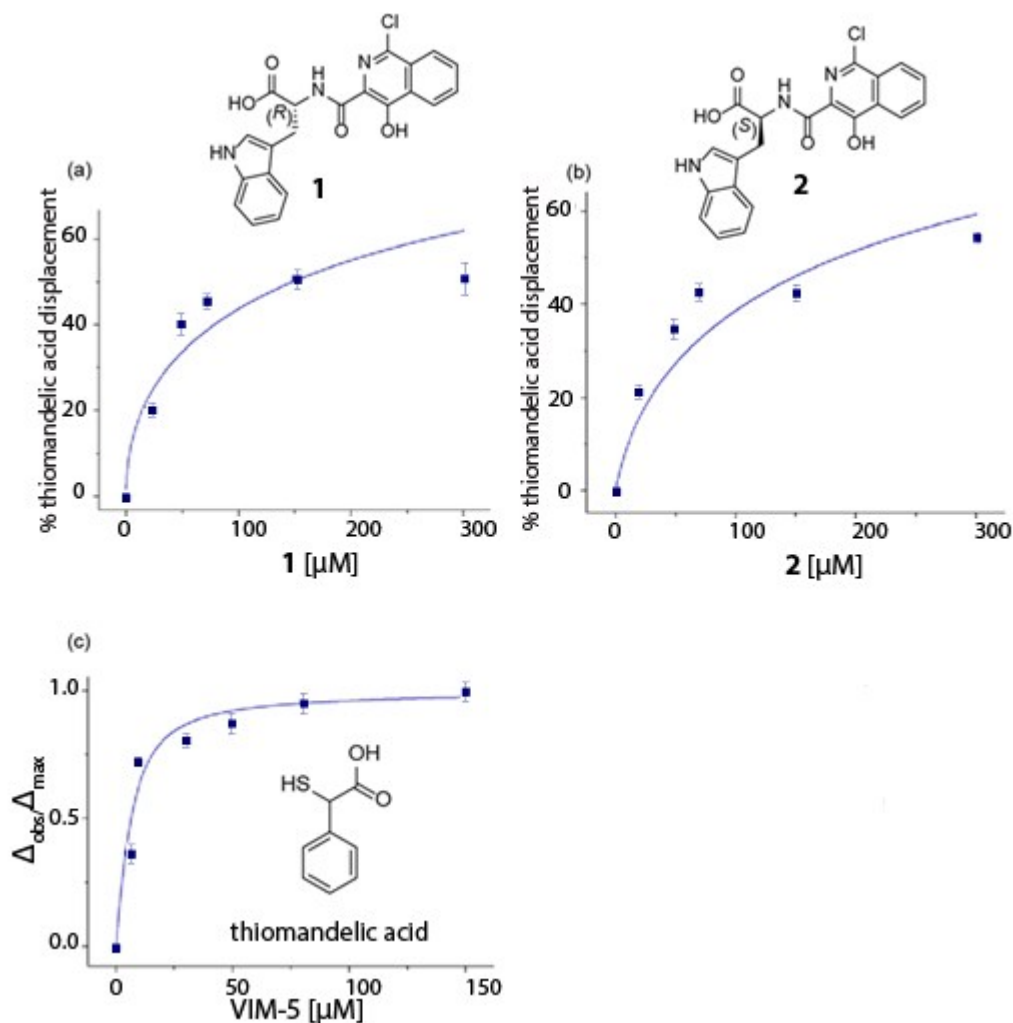


Fig. S9 K_D curve fitting for the binding of compounds **1** and **2** to di-Zn(II)-VIM-5 as observed by ^1H CPMG NMR analyses. (a) and (b) K_D curve fitting for the binding of **1** and **2** to di-Zn(II)-VIM-5 as observed by the displacement of racemic thiomandelic acid by ^1H CPMG. The assay mixture contained 50 μM VIM-5, 100 μM Zn(II), 50 μM thiomandelic acid, buffered with 50 mM Tris- D_{11} , pH 7.5, and 0.02 % NaN_3 in 90 % H_2O and 10 % D_2O . % thiomandelic acid displacement (signal recovery) was plotted against increasing concentrations of **1** or **2** (0-300 μM). (c) K_D curve fitting for the binding of thiomandelic acid to di-Zn(II)-VIM-5 as observed by ^1H CPMG. The assay mixture contained 50 μM thiomandelic acid, buffered with 50 mM Tris- D_{11} , pH 7.5, and 0.02 % NaN_3 in 90 % H_2O and 10 % D_2O , and increasing concentrations of di-Zn(II)-VIM-5 (0-150 μM).

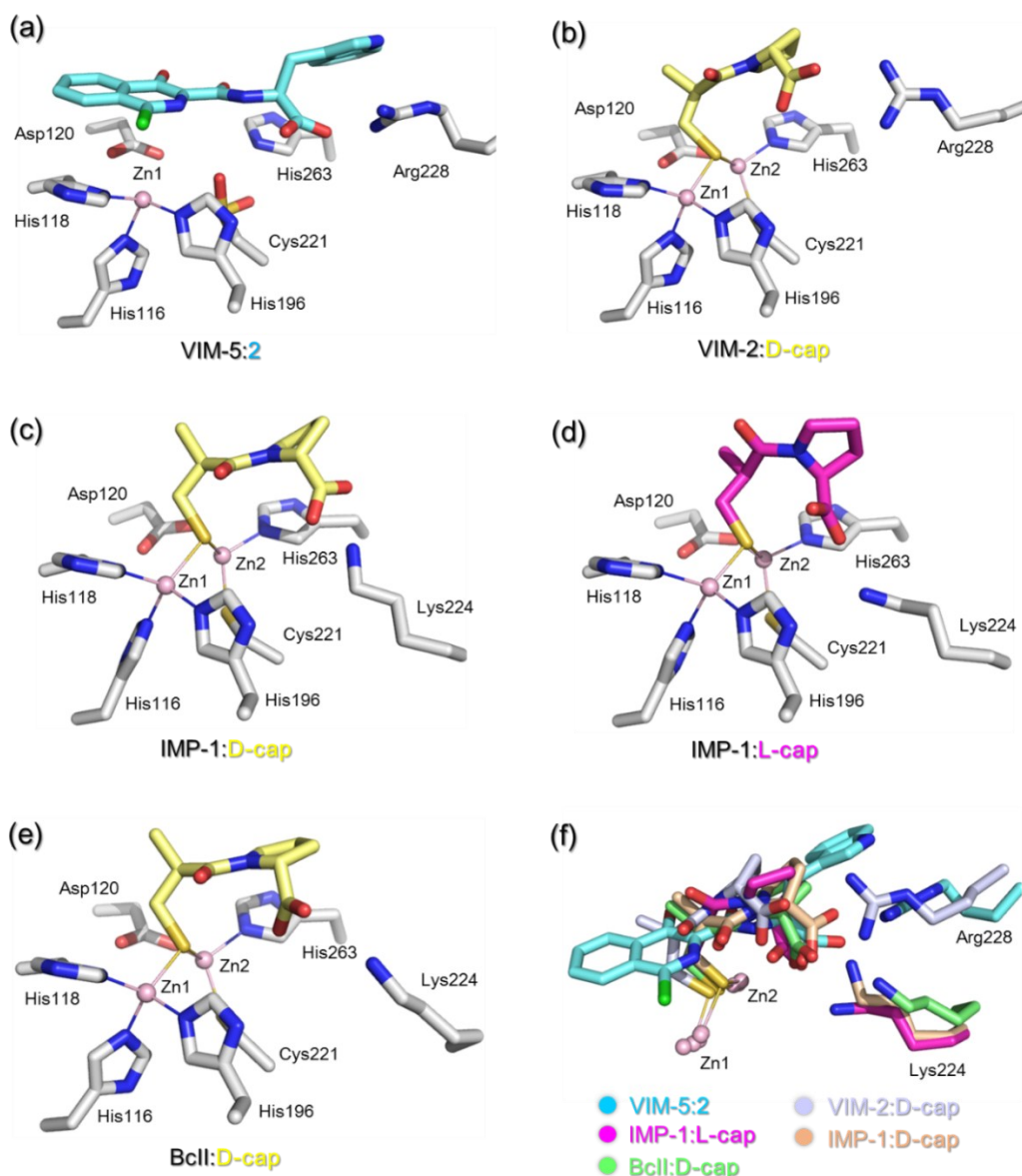


Fig. S10 Comparison of crystal structures of isoquinoline and D-/L-captopril complexed with class B1 MBLs. (a) structure of isoquinoline compound **2** complexed with VIM-5 (PDB ID: 5N55); (b) structure of D-captopril complexed with VIM-2 (PDB ID: 4C1E)¹⁰; (c) structure of D-captopril complexed with IMP-1 (PDB ID: 4C1G)¹⁰; (d) structure of L-captopril complexed with IMP-1 (PDB ID: 4C1F)¹⁰; (e) structure of D-captopril complexed with BclI (PDB ID: 4C1C)¹⁰; (f) superimposition of these crystal structures shown in (a-e). Zinc atoms are represented by pink spheres. The isoquinoline compound **2**, D-captopril and L-captopril ligands are shown in aquamarine, yellow, and magenta, respectively.

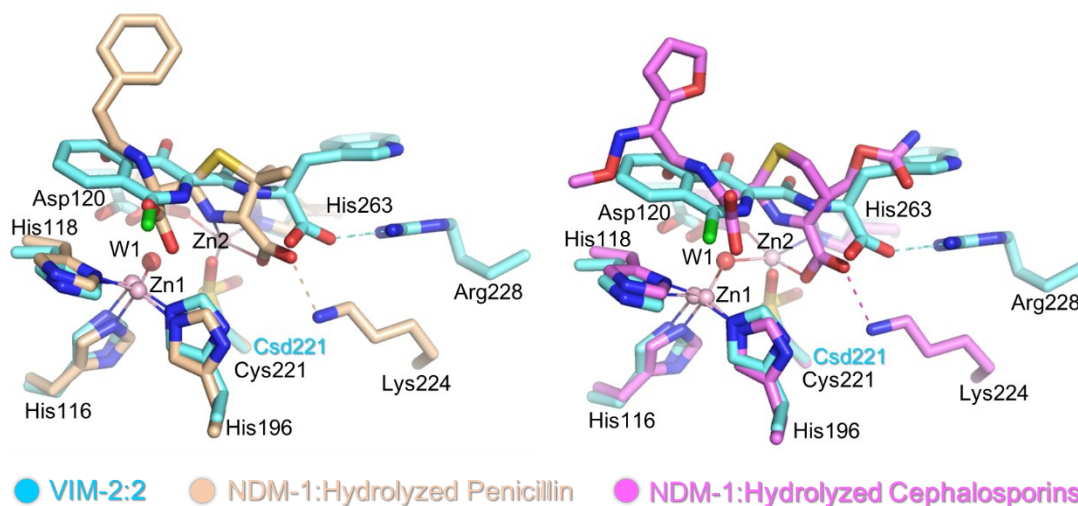


Fig. S11 Comparison of the VIM-5:2 structure (PDB ID: 5N55) with structures of hydrolyzed penicillin (PDB ID: 4EYF)¹⁷ or hydrolyzed cephalosporin (PDB ID: 4RL0)¹⁸ with NDM-1 reveals that **2** binds to VIM-2 via a similar binding mode to that of MBL substrates, e.g. the carboxylate of **2** forms electrostatic interactions with Arg228 (VIM-2), corresponding to equivalent residue Lys224 (NDM-1), which are involved in binding with the substrate carboxylate.

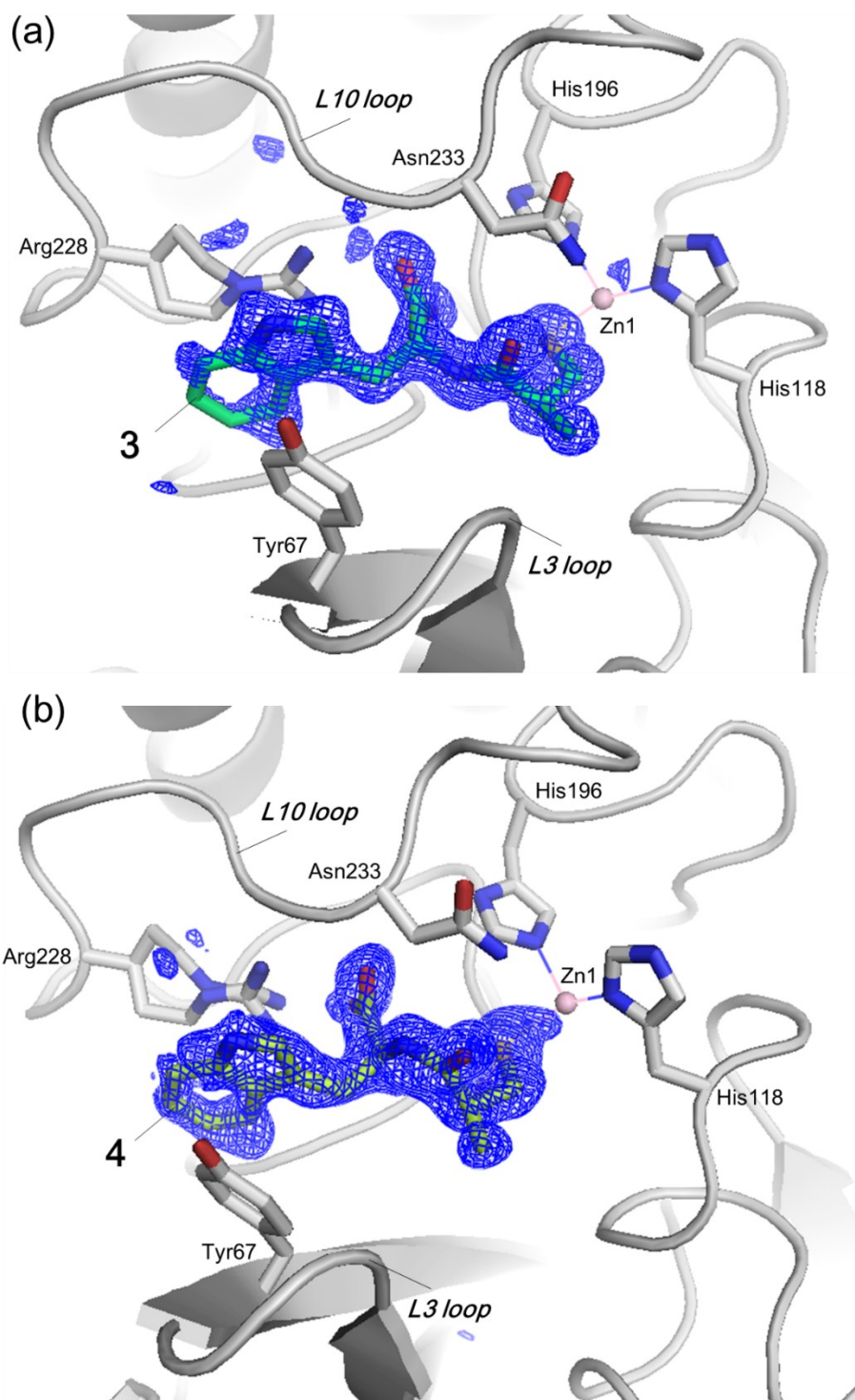


Fig. S12 Binding modes of 3 and 4 as defined by electron density maps. Structures of (a) VIM-2:3 (PDB ID: 5N4S) and (b) VIM-2:4 (PDB ID: 5N4T) (protein and compound colors and representations as in Fig. 4) with the mF_o-DF_c electron density (OMIT maps) around 3 and 4 (blue mesh, contoured to 3σ) calculated from the final refined model without ligand present.

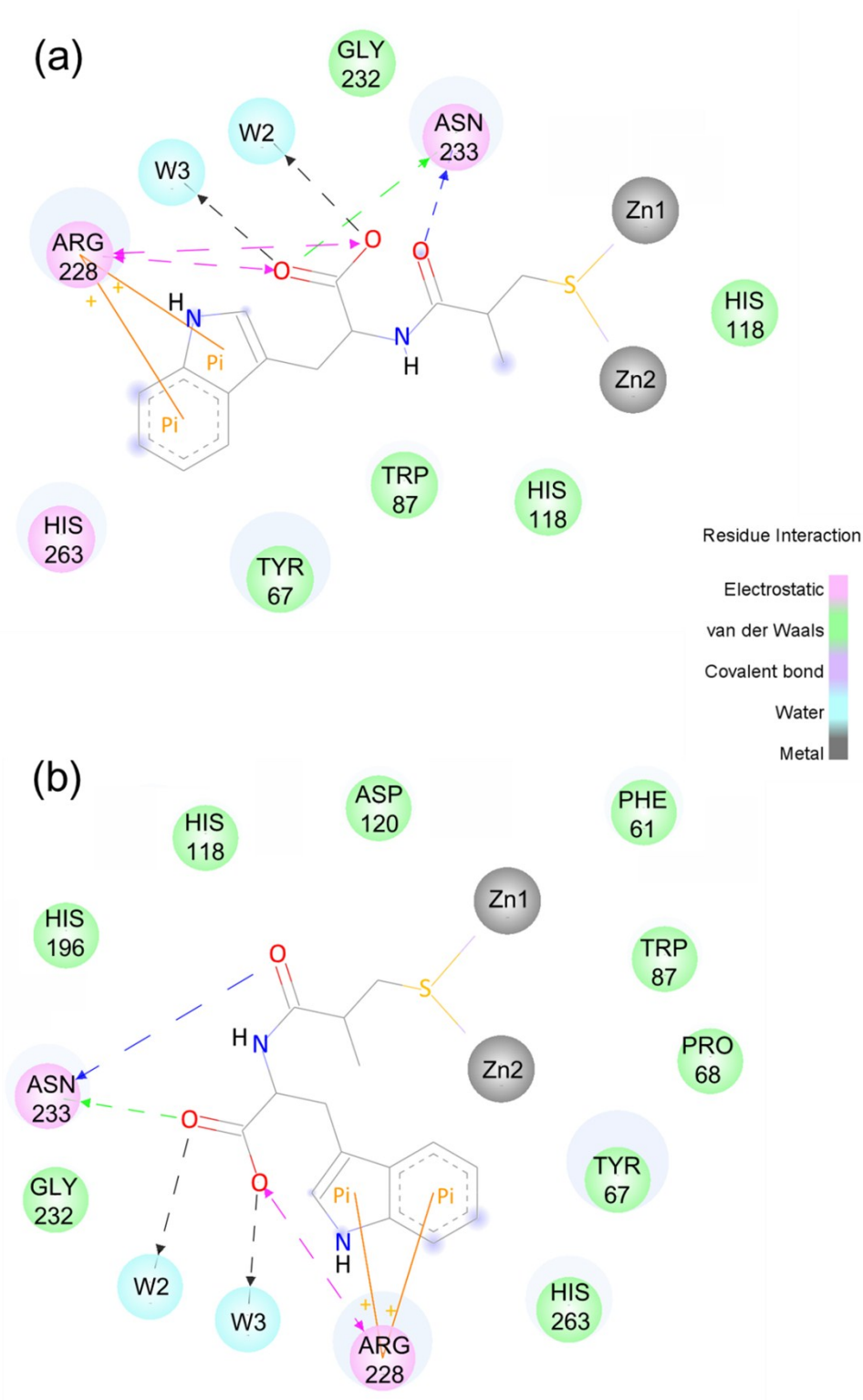


Fig. S13 Protein-ligand interactions between 3 and 4 and VIM-2 as defined using the Discovery Studio Visualizer. Compounds **3** and **4** display very similar binding modes with VIM-2 active site residues. The carboxylates of **3** and **4** are positioned to make hydrogen-bonding and electrostatic interactions with Arg228 and Asn233, the indole moiety is positioned to form cation- π interactions with Arg228, and the thiol group appears chelated with the VIM-2 active site zinc ions.

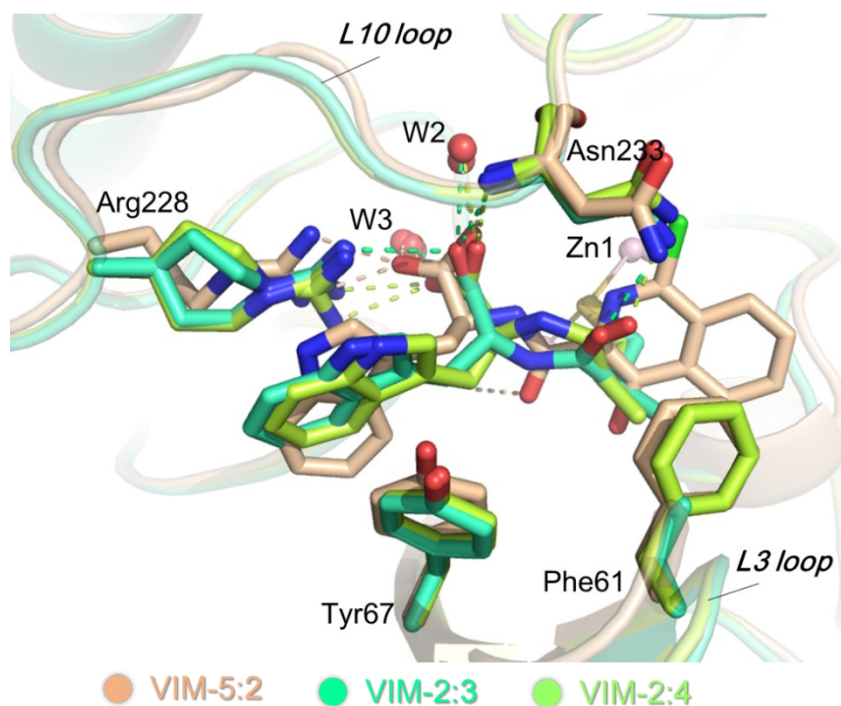


Fig. S14 Comparison of structures of VIM-5:2 (PDB: 5N55), VIM-2:3 (PDB: 5N4S), and VIM-2:4 (PDB: 5N4T) complexes indicates a similar binding mode. The inhibitor carboxylates are positioned to form hydrogen-bonding interactions with Asn233 and Arg228, and the indole moiety is positioned to form cation- π interactions with Arg228, and π - π stacking interactions with Tyr67.

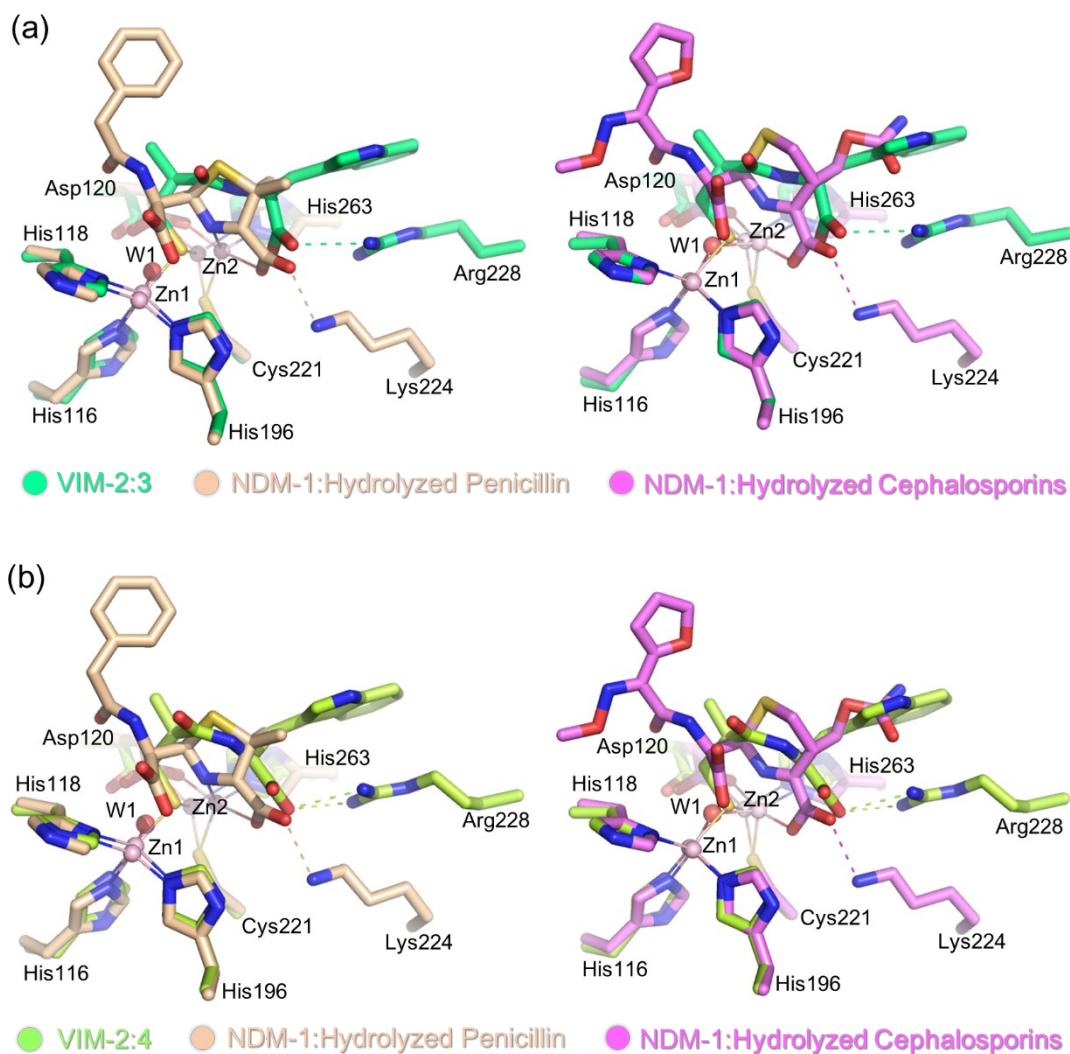


Fig. S15 (a) Comparison of the VIM-2:3 structure (PDB ID: 5N4S) with structures of hydrolyzed penicillin (PDB ID: 4EYF)¹⁷ and hydrolyzed cephalosporin (PDB ID: 4RL0)¹⁸ with NDM-1 reveals that **3** binds via a similar manner to that of MBL hydrolysed penicillin and cephalosporin, e.g. the carboxylate of **2** is positioned to form electrostatic interactions with Arg228 (VIM-2), corresponding to equivalent residue Lys224 (NDM-1), which is involved in binding the substrate carboxylate. (b) Comparison of the VIM-2:4 structure (PDB ID: 5N4T) with structures of hydrolyzed penicillin (PDB ID: 4EYF)¹⁷ or hydrolyzed cephalosporin (PDB ID: 4RL0)¹⁸ with NDM-1 reveals that **4** and **3** bind via in a similar manner to β -lactam substrates.

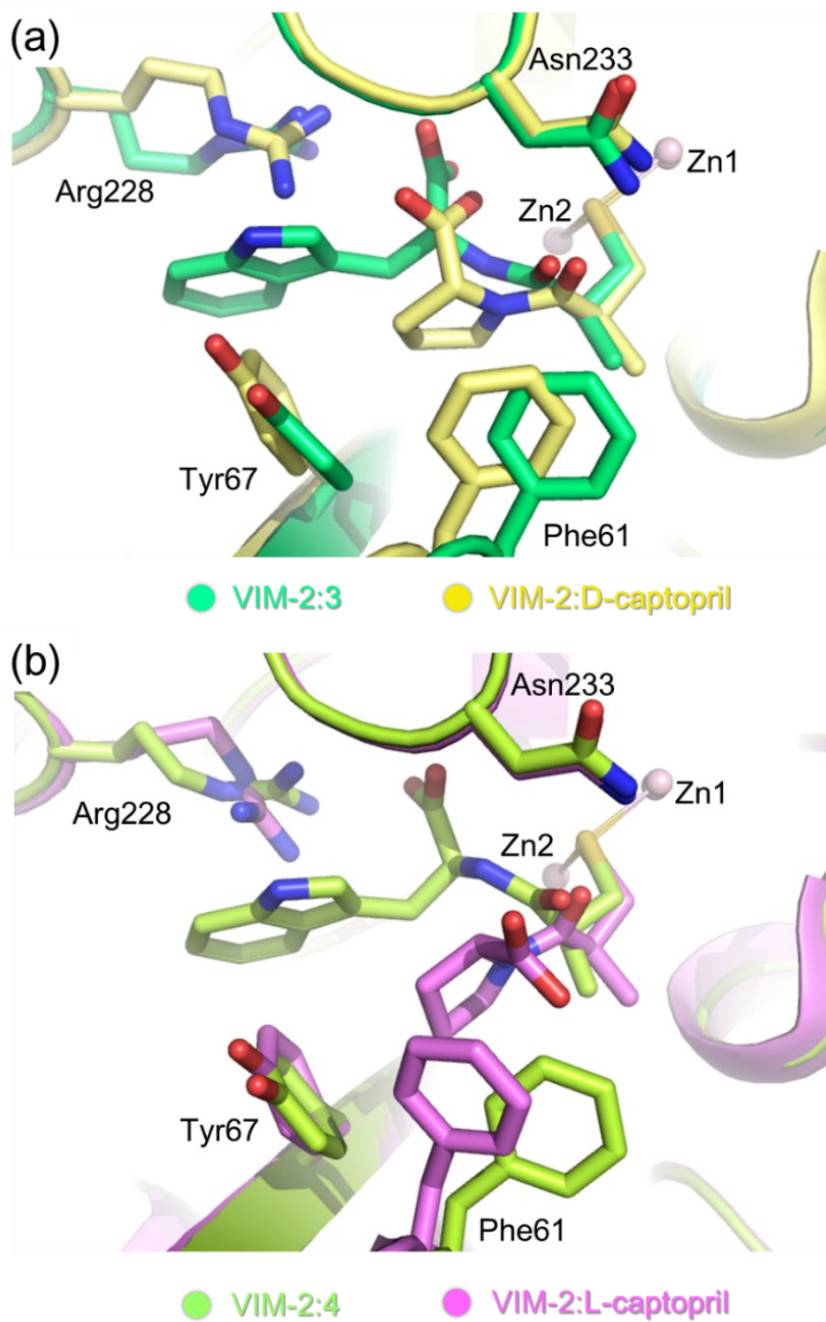


Fig. S16 (a) Comparison of the VIM-2:3 structure (PDB ID: 5N4S) with that of VIM-2:D-captopril (PDB ID: 4C1E)¹⁰ reveals **3** has a very similar binding mode to D-captopril (in particular their amino group); (b) Comparison of the VIM-2:4 structure (PDB ID: 5N4T) with VIM-2:L-captopril (PDB ID: 4C1D)¹⁰ indicates **4** binds similarly to L-captopril.

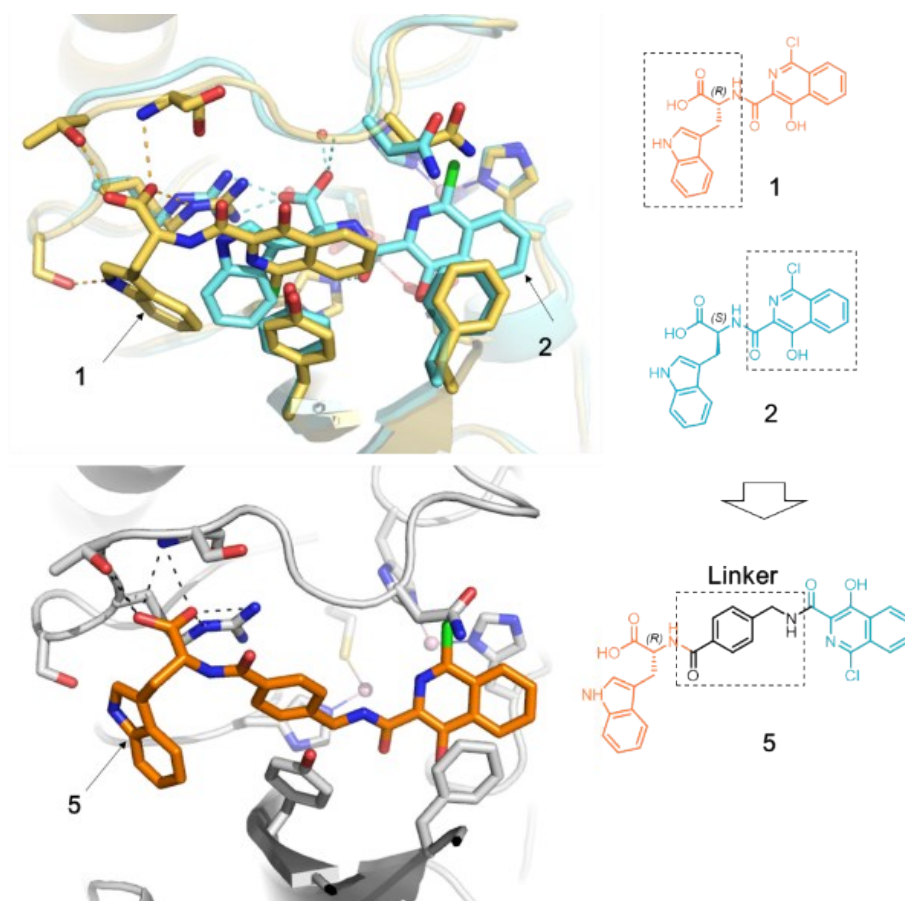


Fig. S17 Design of 5 by linking indole moiety of 1 and isoquinoline ring of 2.

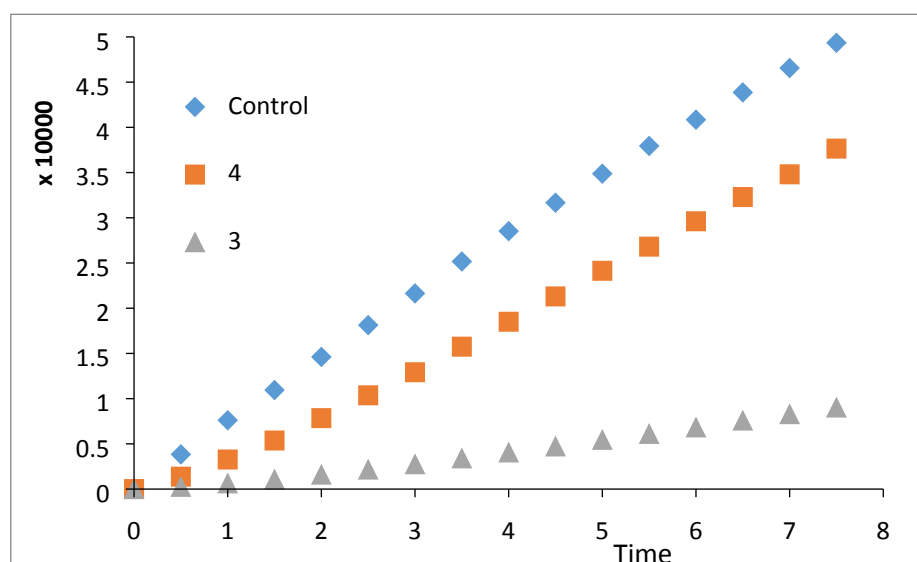


Fig. S18 Testing the reversibility of the inhibition. Recovery of enzyme activity after rapid dilution was tested using the published method.¹⁹ VIM-2 at 10 nM (the enzyme concentration equal to 100-fold used in the activity assay) and 3 at 0.55 μ M and 4 at 10 μ M (i.e. the concentrations of inhibitor equal to 10-fold the IC_{50} value) were pre-incubated (30 min at r.t.). The samples were then rapidly diluted (100 fold) and the enzyme activity was measured.

Table S2. Crystallography conditions.

Structure	Method	Sample composition ^a	Crystallization condition	Vapour diffusion condition
VIM-5:1	Co-crystallization	VIM-5 in crystallization buffer + TCEP (1 mM) + inhibitor 1 (5 mM)	0.02 M Sodium/potassium phosphate, 0.1 M Bis-Tris propane, 20% (w/v) Polyethylene glycol 3350, pH=6.5	Sitting drop, protein-to-well ratio, 1:1, 293K
VIM-5-OX:1	Co-crystallization	VIM-5 in crystallization buffer + TCEP (1 mM) + inhibitor 1 (5 mM)	0.2 M Sodium fluoride, 0.1 M Bis-Tris propane, 20% (w/v) Polyethylene glycol 3350, pH=8.5	Sitting drop, protein-to-well ratio, 1:2, 293K
VIM-5:2	Co-crystallization	VIM-5 in crystallization buffer + TCEP (1 mM) + inhibitor 2 (5 mM)	0.2 M Lithium Chloride, 0.1 M 2-(N-morpholino)ethane sulfonic acid (MES), 20% (w/v) Polyethylene glycol 6000, pH=6.0	Sitting drop, protein-to-well ratio, 1:1, 293K
VIM-2:3	Socking	Crystal + TCEP (1 mM) + inhibitor 3 (10mM) + 25% (v/v) Glycerol for about 6 hours	0.1 M Magnesium Formate, 21%~27% (v/v) Polyethylene glycol 3350	Sitting drop, protein-to-well ratio, 1:1, 293K
VIM-2:4	Socking	Crystal + TCEP (1 mM) + inhibitor 4 (10mM) + 25% (v/v) Glycerol for about 6 hours	0.1 M Magnesium Formate, 21%~27% (v/v) Polyethylene glycol 3350	Sitting drop, protein-to-well ratio, 1:1, 293K

^aCrystallization buffer = 50mM 4-(2-hydroxyethyl)-1-piperazineethanesulfonic acid (HEPES) pH 7.5 + 100 mM NaCl; TECP = tris(2-carboxyethyl)phosphine.

Table S3. Data collection and refinement statistics.

Structure	VIM-5:1	VIM-5-OX:2	VIM-5-OX:1	VIM-2:3	VIM-2:4
PDB ID	5N58	5N55	5NAI	5N4S	5N4T
Processing					
Radiation Source	I04	I04	I04	I04	I04
Space Group	$P 2_1 2_1 2_1$	$F 2 2 2$	$P 1 2_1 1$	$C 1 2 1$	$C 1 2 1$
Unit Cell Dimensions a, b, c (Å)	54.471 81.540 95.892	66.2195 155.191 267.733	39.55 67.555 40.09	103.845 80.308 68.732	105.903 80.148 79.085
Unit Cell Dimensions α, β, γ (°)	90.00 90.00 90.00	90.00 90.00 90.00	90.00 92.66 90.00	90.00 130.34 90.00	90.00 139.49 90.00
*Mol/ASU	2	3	1	2	2
Resolution Range (outer shell) (Å)	62.12-1.96 (2.02-1.96)	50.68-1.99 (2.02-1.99)	50.00-1.15 (1.19-1.15)	52.21-1.20 (1.22-1.20)	56.29-1.16 (1.20-1.16)
Number of Unique Reflections	31256	47393	72606	131443	146189
Completeness (%)	99.19	99.58	99.99	98.33	99.46
$I/\sigma(I)$ (outer shell)	14.3 (1.9)	15.3 (2.1)	24.9 (2.67)	9.0 (1.3)	10.3 (1.4)
R_{merge} (outer shell)	15.2 (149.2)	9.8 (119.7)	7.0 (17.4)	9.4 (138.7)	7.3 (127.7)
Wilson B Factor (Å ²)	23.6	23.61	14.87	8.4	9.7
Refinement					
Overall B Factor (Å ²)	33.81	31.22	19.90	18.32	20.03
Protein B Factor (Å ²)	33.18	31.07	18.22	16.44	17.20
Ligand B Factor (Å ²) (occupancy)	46.61 (1.0)	35.66 (1.0)	19.89 (1.0)	27.89 (1.0)	31.43 (1.0)
Water B Factor (Å ²)	39.32	32.49	35.46	30.29	31.37
‡RMSD from Ideal Bond Length (Å)	0.016	0.014	0.007	0.010	0.010
RMSD from Ideal Angles (°)	1.075	1.094	1.010	1.020	1.010
R_{work} (%)	18.74	19.14	13.28	18.40	17.45
R_{free} (%)	23.72	25.26	14.16	20.02	19.67

*Mol/ASU = molecules per asymmetric unit; ‡RMSD = root mean square deviation.

Reference

- 1 C. Dalvit, P. Pevarello, M. Tato, M. Veronesi, A. Vulpetti and M. Sundstrom, *J. Biomol. NMR*, 2000, **18**, 65.
- 2 J. A. Aguilar, M. Nilsson, G. Bodenhausen and G. A. Morris, *Chem. Commun.*, 2012, **48**, 811.
- 3 A. Makena, A. Ö. Düzgün, J. Brem, M. A. McDonough, A. M. Rydzik, M. I. Abboud, A. Saral, A. Ç. Çiçek, C. Sandalli and C. J. Schofield, *Antimicrob. Agents Chemother.*, 2016, **60**, 1377.
- 4 S. S. van Berkel, J. Brem, A. M. Rydzik, R. Salimraj, R. Cain, A. Verma, R. J. Owens, C. W. Fishwick, J. Spencer and C. J. Schofield, *J. Med. Chem.*, 2013, **56**, 6945.
- 5 L. Horsfall, G. Garau, B. Liénard, O. Dideberg, C. Schofield, J. Frere and M. Galleni, *Antimicrob. Agents Chemother.*, 2007, **51**, 2136.
- 6 L. Nauton, R. Kahn, G. Garau, J.-F. Hernandez and O. Dideberg, *J. Mol. Biol.*, 2008, **375**, 257.
- 7 A. J. McCoy, R. W. Grosse-Kunstleve, P. D. Adams, M. D. Winn, L. C. Storoni and R. J. Read, *J. Appl. Crystallogr.*, 2007, **40**, 658.
- 8 P. D. Adams, P. V. Afonine, G. Bunkoczi, V. B. Chen, I. W. Davis, N. Echols, J. J. Headd, L. W. Hung, G. J. Kapral, R. W. Grosse-Kunstleve, A. J. McCoy, N. W. Moriarty, R. Oeffner, R. J. Read, D. C. Richardson, J. S. Richardson, T. C. Terwilliger and P. H. Zwart, *Acta Crystallogr. D Biol. Crystallogr.*, 2010, **66**, 213.
- 9 J. Brem, S. S. van Berkel, W. Aik, A. M. Rydzik, M. B. Avison, I. Pettinati, K.-D. Umland, A. Kawamura, J. Spencer, T. D. Claridge, M. A. McDonough and C. J. Schofield, *Nat. Chem.*, 2014, **6**, 1084.
- 10 J. Brem, S. S. van Berkel, D. Zollman, S. Y. Lee, O. Gileadi, P. J. McHugh, T. R. Walsh, M. A. McDonough and C. J. Schofield, *Antimicrob. Agents Chemother.*, 2016, **60**, 142.
- 11 P. Emsley and K. Cowtan, *Acta Crystallogr. D Biol. Crystallogr.*, 2004, **60**, 2126.
- 12 M. B. Avison, S. Underwood, A. Okazaki, T. R. Walsh and P. M. Bennett, *J. Antimicrob. Chemother.*, 2004, **53**, 584.
- 13 R. G. Forage and E. C. Lin, *J. Bacteriol.*, 1982, **151**, 591.
- 14 B. Bartolome, Y. Jubete, E. Martinez and F. de la Cruz, *Gene*, 1991, **102**, 75.
- 15 Methods for Dilution Antimicrobial Susceptibility Tests for Bacteria That Grow Aerobically; Approved Standard, 10th edn. M07-A10. CLSI, American Society for Microbiology, USA, 2015.
- 16 Clinical and Laboratory Standards Institute. Performance Standards for Antimicrobial Susceptibility Testing: Twenty-fourth Informational Supplement M100-S24. CLSI, Wayne, PA, USA, 2014.
- 17 D. T. King, L. J. Worrall, R. Gruninger and N. C. J. Strynadka, *J. Am. Chem. Soc.*, 2012, **134**, 11362.
- 18 H. Feng, J. Ding, D. Zhu, X. Liu, X. Xu, Y. Zhang, S. Zang, D. C. Wang and W. Liu, *J. Am. Chem. Soc.*, 2014, **136**, 14694..
- 19 R. A. Copeland, Evaluation of Enzyme Inhibitors In Drug Discovery, Wiley, 2013.